Rev. Roum. Sci. Techn.– Électrotechn. et Énerg.
Vol. **63**, *1*, pp. 38–45, Bucarest, 2018

A MODIFIED DIRECT TORQUE CONTROL FOR INDUCTION MOTOR DRIVES

NOURI BELHAOUCHET, HICHEM HAMLA, LAZHAR RAHMANI

Key words: Direct torque control (DTC), Hysteresis current control (HCC), Space vector modulation (SVM), Induction motor, Switching losses.

This paper presents a modified direct torque control based on combination of hysteresis current control and space vector modulation for induction motor drives. This technique is characterized by simplicity and high performance flux and torque control in ac drive systems. The configuration of hysteresis current control and space vector modulation in direct torque control technique can reduce drastically the switching losses by implementing space vector modulation technique and produce a better stator current waveform by using a significant tolerance bandwidth of the hysteresis current control. The behavior of the proposed technique is fully verified by digital simulation using Matlab/Simulink and experimental implementation on dSPACE 1 104 system card.

1. INTRODUCTION

In the past, electrical motors speed regulations were realized with dc motors because their easy control. However, it is well known that this kind of motors presents several disadvantages as higher cost of buying, higher rotor inertia and maintenance problem with commutators and brushes. In addition they cannot operate in dirty and explosive environments. That's why in last few decades the dc motors are progressively replaced by ac drives especially with induction motors, which have good economic aspects, and a high power/size report. The responsible for those results are the development of modern semiconductor devices and the digital signal processor technologies.

The most economical induction motors speed control methods are realized by using frequency converters. Many different topologies of frequency converters are proposed and investigated in the literature. However, a converter consisting of a diode rectifier, a dc link and a pulse width modulated (PWM) voltage inverter is the most applied in industry. The high-performance frequency controlled PWM inverter fed induction motor drive should be characterized by fast flux and torque response, available maximum output torque in wide range of speed operation region, constant switching frequency, unipolar voltage PWM, low flux and torque ripple, robustness for parameter variation, four-quadrant operation [1].

These features depend on the applied control technique. The main objective of the chosen control method is to provide the best possible performances of the drive, with low cost and without complexity. Induction motor control methods can be divided into scalar and vector control, where the general classification of the variable-frequency methods is presented in [1, 2]. In the control of electrical drives there are two main control schemes that have dominated high-performance applications during the last few decades: (1) field oriented control (FOC), in which a decoupled torque and flux control is performed by considering an appropriate coordinate frame; (2) a nonlinear hysteresis-based strategy such as direct torque control (DTC), which appears to be a solution for high performance applications.

Over the past years, DTC scheme for induction motor drives has received enormous attention in industrial motor drive applications. The main reason for its popularity is due to its simple structure, particularly when compared with FOC scheme. The DTC is one of the actively researched control techniques which is based on the decoupled control of stator flux and torque providing a quick and robust response with a simple control construction in ac drives. This technique is derived from the fact, that on the basis of the errors between the reference and the estimated values of torque and flux, it is possible to control directly the inverter states in order to reduce the torque and flux errors within pre-fixed band limits.

The major disadvantages of DTC technique using hysteresis controllers are variable switching frequency, difficulty to control torque and flux at very low speed, high current and torque ripple, high noise level at low speed and absence of direct current control. During the last three decades, a variety of modifications have been made to overcome some drawbacks present in conventional DTC technique. The objective of these modifications was to improve the start up of the motor, the operation in overload conditions and low speed region. The modifications also aimed to reduce the torque and current ripple, the noise level and to avoid the variable switching frequency [3–14].

This paper proposes a modified DTC based on combination of hysteresis current control (HCC) and space vector modulation (SVM) techniques. The fundamental idea of the proposed method is to control not only the torque and the stator flux but also the stator currents with reduced switching losses. Indeed, its principle is very simple, the conventional DTC maintains its analog structure, but a modification is brought which ensures the control of stator currents by using HCC technique. The HCC is very suitable for current control, but it generates other vectors than the space vectors required according to the region in the SVM technique. For this reason, by implementing of SVM technique which limits the space vectors to be applied according to the region where the reference output voltage vector is located, a considerably reduction of switchings number is obtained. Thus, by combining both SVM and HCC techniques in DTC, the disadvantages can be distinctly reduced and the ac drive performances can be noticeably improved.

The remaining contents of this paper are organized as follows. Section 2 introduces the conventional DTC scheme principle based on switching look-up table. Sections 3 and 4 describe respectively the basic operating principles of

University Ferhat Abbas, Faculty of Technology, Laboratory of Automatic, Electrical Engineering Department, SETIF-1, Algeria, E-mail : nouri_belhaouchet@yahoo.fr; hamla_hichem@yahoo.fr; lazhar_rah@yahoo.fr

DTC based on HCC and proposed DTC based on combination of HCC and SVM. Section 5 discusses the simulation results obtained by using MATLAB/SIMULINK software in steady and dynamic states for conventional DTC and proposed DTC based on combination of HCC and SVM. Section 6 presents the experimental implementation on dSPACE 1 104 system card and the obtained experimental results of both methods. Conclusions are finally drawn in the last section.

2. CONVENTIONAL DTC PRINCIPLE

The behavior of induction motor in DTC drives can be described in terms of space vectors by the following equations written in stator stationary reference frame [5].

$$v_s = R_s i_s + \frac{\mathrm{d}\psi_s}{\mathrm{d}t} \tag{1}$$

$$0 = R_r i_r + \frac{\mathrm{d}\psi_r}{\mathrm{d}t} - j\omega_m \psi_r \tag{2}$$

$$\psi_s = L_s i_s + L_m i_r \tag{3}$$

$$\psi_r = L_m i_s + L_r i_r \tag{4}$$

$$T_{em} = p \frac{L_m}{\sigma L_s L_r}\left(\psi_s . j\psi_r\right), \tag{5}$$

with:

$$\sigma = 1 - L_m^2 / L_s L_r .$$

The equation of the dynamic rotor rotation can be expressed as:

$$J \frac{\mathrm{d}\Omega}{\mathrm{d}t} = T_{em} - T_L , \tag{6}$$

where: v_s stator voltage vector, i_s stator current vector, i_r – rotor current vector, R_s – stator resistance, R_r – rotor resistance, L_m – mutual inductance, L_s – stator inductance, L_r – rotor inductance, ψ_s – stator flux vector, ψ_r – rotor flux vector, ω_m – rotor electric speed, T_{em} – electromagnetic torque, p – number of pairs of poles, σ – leakage coefficient, J – inertia, Ω – mechanical speed, T_L – load torque.

Basically, DTC schemes require the estimation of the stator flux and torque. The stator flux evaluation can be carried out by different techniques depending on whether the rotor angular speed or (position) is measured or not. For sensorless application, the "voltage model" is usually employed.

Considering the combination of states of switching functions (S_1, S_2, S_3), dc link voltage V_{dc} and stator current measurements; the stator flux can be evaluated by integrating from the stator voltage equation

$$\psi_s(t) = \int \left(v_s - R_s i_s\right)\mathrm{d}t . \tag{7}$$

For calculation of flux using (7), voltage vectors are required which can be derived by first calculating the phase voltages and then converting them in two phase quantity in a stationary reference frame.

$$\begin{bmatrix} v_{sa} \\ v_{sb} \\ v_{sc} \end{bmatrix} = \frac{V_{dc}}{3}\begin{bmatrix} 2 & -1 & -1 \\ -1 & 2 & -1 \\ -1 & -1 & 2 \end{bmatrix}\begin{bmatrix} S_1 \\ S_2 \\ S_3 \end{bmatrix} \tag{8}$$

$$\begin{bmatrix} v_\alpha \\ v_\beta \end{bmatrix} = \frac{V_{dc}}{3}\begin{bmatrix} 2 & -1 & -1 \\ 0 & \sqrt{3} & -\sqrt{3} \end{bmatrix}\begin{bmatrix} S_1 \\ S_2 \\ S_3 \end{bmatrix}, \tag{9}$$

where v_{sa}, v_{sb} and v_{sc} denote phase voltages; S_1, S_2, S_3 denote inverter switching states, $S_k = 1$ (k = 1, 2, 3), if the upper leg switch is on and $S_k = 0$, if the lower leg switch is on; v_α and v_β are α and β axis stator voltage in stationary reference frame.

This method is very simple requiring only the knowledge of the stator resistance. The effect of an error in R_s is usually quite negligible at high excitation frequency but becomes more serious as the frequency approaches zero. The electromagnetic torque is estimated from the flux and current as:

$$T_e = p(i_{s\beta}\psi_{s\alpha} - i_{s\alpha}\psi_{s\beta}) . \tag{10}$$

The stator flux angle θ_s is calculated from the estimated stator flux ψ_s in the reference frame related to the stator

$$\theta_s = \arctan(\psi_{s\beta} / \psi_{s\alpha}) . \tag{11}$$

The block diagram of the basic DTC scheme is shown in Fig. 1. The principle of the conventional DTC is based on its decoupled control of stator flux and electromagnetic torque [5–9]. The error between the estimated torque T_e and the reference torque T_e* is the input of a two-level hysteresis comparator, also the error between the estimated stator flux magnitude $|\psi_s|$ and the reference stator flux magnitude $|\psi_s{*}|$ is the input of a two level-hysteresis comparator. A switching look-up table is included for selection of the appropriate voltage vector for three-phase inverter feeding the induction motor. This simple approach offers high performance in terms of simplicity in control and fast electromagnetic torque response, but the steady state performance is characterized by undesirable ripple in the flux and torque. Moreover, it does not allow the direct control of stator currents.

3. OPERATING PRINCIPLE OF DTC BASED ON HCC

The HCC technique is characterized by its easy implementation, fast dynamic response, inherent peak current limiting capability, and insensitivity to load parameters variation. The basic idea of HCC is to keep the current inside the hysteresis band by changing the switching state of the converter each time the current reaches the boundary. This current control technique plays the most important role in current-controlled PWM inverters, which are widely applied in high-performance ac drives [15–17] and harmonic compensation systems [18].

The operation of a three-phase voltage-source inverter (VSI) feeding an ac motor is described with reference to Fig. 2, where the motor load is represented by a symmetrical approximated equivalent scheme including R_s, L_{ls} impedances and back-emf's.

Referring to the topology of Fig. 2, the relationship between phase voltage vector and load current vector can be formulated as:

$$v_s = R_s i_s + L_{ls}\frac{\mathrm{d}i_s}{\mathrm{d}t} + e . \tag{12}$$

For a reference load current vector i_s*, consequently, the reference phase voltage vector may be defined as:

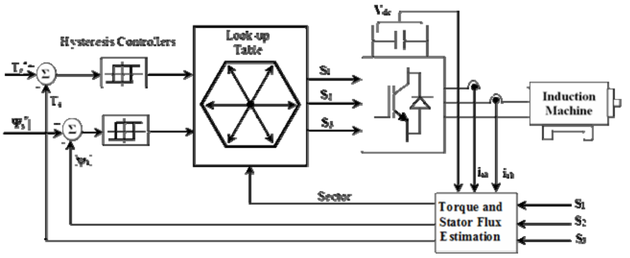

Fig. 1 – Block diagram of basic DTC scheme.

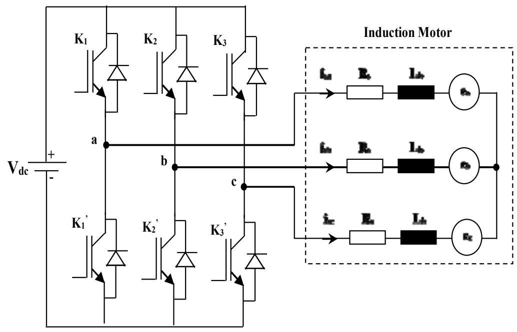

Fig. 2 – Voltage source inverter feeding induction motor.

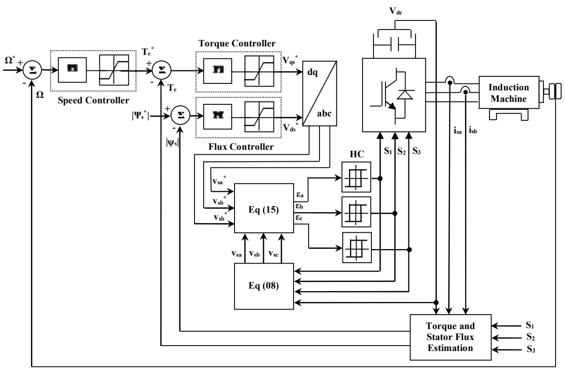

Fig. 3 – Block diagram of the DTC based on HCC scheme.

$$v_s^* = R_s i_s^* + L_{ls} \frac{\mathrm{d}i_s^*}{\mathrm{d}t} + e \,. \tag{13}$$

The instantaneous current error vector is the deviations between the actual current vector and the reference current vector as:

$$\varepsilon = i_s^* - i_s \,. \tag{14}$$

So from (12), (13) and (14), one can write:

$$L_{ls} \frac{\mathrm{d}\varepsilon}{\mathrm{d}t} + R_s \varepsilon = v_s^* - v_s \,. \tag{15}$$

The DTC based on HCC developed in this work (Fig. 3) is similar to conventional DTC based on hysteresis comparators and switching look-up table (Fig. 1). For the developed technique proportional-integral controllers can replace the hysteresis comparators for torque and flux control, and instead of using switching look-up table, a current error for each phase is deduced from equation (15), and then is sent to hysteresis current comparator (HC) in order to generate the switching pulses and ensure the control of stator currents. The phase voltages are estimated from the dc link voltage V_{dc} and the states of inverter switches according to (8). The advantage of this modified DTC compared to conventional DTC based on switching look-up table is to control not only the torque and the magnitude of flux but also the stator currents.

4. OPERATING PRINCIPLE OF DTC BASED ON COMBINATION OF HCC AND SVM

The HCC technique plays an important role in fast response current controlled PWM inverters. This technique provides instantaneous current corrective response, good accuracy and unconditioned stability to the system. Besides that, this technique is said to be the most suitable solution for current controlled PWM inverters. However, due to a heavy interaction between the phases when the neutral is insulated to the dc link midpoint, a highly switching frequency variation may occur and the current error is not strictly limited by the hysteresis band. These drawbacks provide high current ripples, acoustic noise and difficulty in filtering. In addition, the HCC generates other vectors than the space vectors required according to the region in the SVM technique, which increases the number of switchings and consequently the switching losses [19, 20]. This problem in the HCC can be solved using the space vector concept.

The basic principle of the SVM technique is that it treats the PWM inverter as a whole unit, which is different when compared to sinusoidal PWM technique [21]. This technique is based on the decomposition of a reference voltage vector into voltage vectors realizable on six-pulse PWM inverter which is shown in Fig. 2. However, by applying this concept to six-pulse PWM inverter, eight possible output voltage vectors are available where two of them are the null voltage vectors while the remaining six vectors are 60° apart of each other. The space vectors can be obtained and defined based on the voltage waveform and region division. The PWM inverter can operate with eight switching states, where each state corresponds to a space vector.

The following active space vectors are obtained:

$$V_i = \frac{2}{3} V_{dc} e^{j(i-1)\frac{\pi}{3}}, \quad i = 1,2,...,6. . \tag{16}$$

The available space voltage vectors according to eight switch states are shown in Fig. 4, where the null voltage vector has two switching patterns $V_0(000)$ and $V_0(111)$. The reference output space vector v_s* is obtained from α–β transformation of reference phase voltages. In SVM technique, the conduction times of the switches are modulated according to the magnitude and angle of v_s*. The angle of v_s* determines a region among six regions in the complex plane.

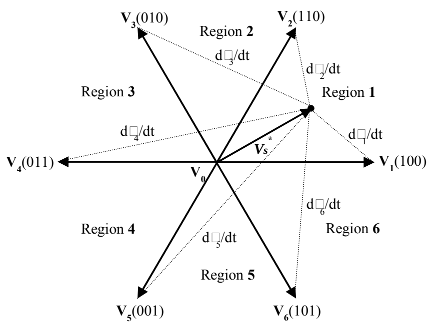

Fig. 4 – Derivative vectors of current error in region 1.

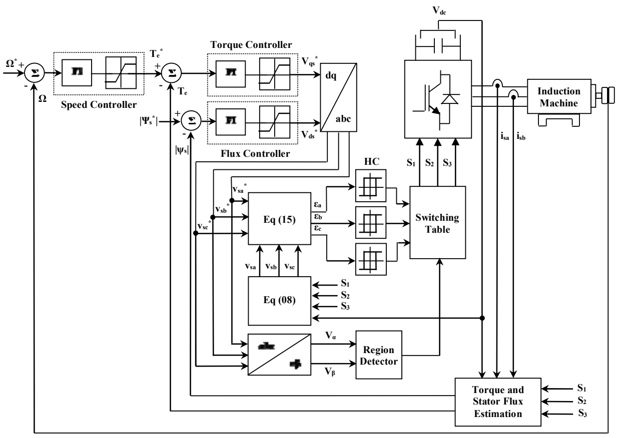

Fig. 5 – Block diagram of the DTC based on combination of HCC and SVM scheme.

Table 1

Switching table for the proposed DTC based on combination of HCC and SVM

Region	HC_1 HC_2 HC_3	V_i
1	1 0 0	V_1
	1 1 0	V_2
	Other cases	V_0
2	1 1 0	V_2
	0 1 0	V_3
	Other cases	V_0
3	0 1 0	V_3
	0 1 1	V_4
	Other cases	V_0
4	0 1 1	V_4
	0 0 1	V_5
	Other cases	V_0
5	0 0 1	V_5
	1 0 1	V_6
	Other cases	V_0
6	1 0 1	V_6
	1 0 0	V_1
	Other cases	V_0

Usually, the effects of the term $R_s.\varepsilon$ can be neglected, so (15) becomes:

$$L_{ls}\frac{\mathrm{d}\varepsilon}{\mathrm{d}t}=v_s^*-v_s\,. \tag{17}$$

The phase voltage v_s is represented by the quantized space vector V_i. Then (17) becomes as follows:

$$L_{ls}\frac{\mathrm{d}\varepsilon}{\mathrm{d}t}=v_s^*-V_i\,. \tag{18}$$

From (18), the derivative vector $\mathrm{d}\varepsilon/\mathrm{d}t$ of the current error determines the desired space voltage vectors V_i for each state. If the reference output space voltage vector v_s* is located in region 1 (Fig. 4), the derivative vectors of the current error with respect to the reference output space voltage vector in region 1 show that $\mathrm{d}\varepsilon_1/\mathrm{d}t$ and $\mathrm{d}\varepsilon_2/\mathrm{d}t$ provide the minimum values of derivative vectors of the current error. Hence, the adequate space voltage vectors for v_s* are V_1, V_2 and V_0. Based on the SVM principles, only correct and adequate vectors are applied in each switching state. By implementing this technique to the HCC, the unnecessary number of switchings can be reduced.

Figure 5 shows the block diagram of the proposed DTC based on combination of HCC and SVM technique for three-phase PWM inverter. The concept of this control employs a very simple structure with the same structure of DTC based on HCC (Fig. 3), but a region detector from the position of the reference space voltage vector and a switching table are added. The hysteresis comparators HC_1, HC_2 and HC_3 are used to limit the current error within a specified band. The space vectors V_0, V_1 and V_2 in region 1 are utilized as in the SVM technique. When HC_1 provides 1, HC_2 provides 0 and HC_3 provides 0, the vector V_1 is applied. On the other hand, V_2 is applied when HC_1 provides 1, HC_2 provides 1 and HC_3 provides 0. In the other cases, the null voltage vector is applied. The region detector and the output signals of the hysteresis comparators, HC_1, HC_2, HC_3, provide the information to a switching look-up table to produce appropriate gate switching signals to the three-phase PWM inverter (Table 1).

5. SIMULATION RESULTS

The parameters of the squirrel-cage induction machine used in simulation and implementation tests are given in Table 2. Note that the stator induction motor is WYE connected. The sampling frequency used for all simulation tests is 20 kHz, the dc voltage source is equal to 630 V and the magnitude of reference stator flux is fixed to the rated value 0.94 Wb.

In conventional DTC, for the flux, a hysteresis band controller of 0.02 Wb was chosen, which is almost 2 % of the rated flux; for the torque, the hysteresis band controller was chosen to be 0.036 Nm, which means 1 % of the rated torque. These adjustments led to an average switchings number of inverter states in rated state equal to 33 960 per second, while for the proposed DTC based on combination of HCC and SVM, the hysteresis bands of current errors equal to 0.2 A were chosen, namely 34620 switching states per second.

The tests, in simulation studies, were conducted to verify feasibility and performance of the proposed DTC based on combination of HCC and SVM compared to the conventional DTC. For these tests, the induction motor operates with a rated speed 2 880 rpm for no-load from 0 to 0.6 s, then for full load of 3.31 Nm from 0.6 s to 1 s.

The waveforms of estimated stator flux magnitude, motor speed and estimated electromagnetic torque, for the conventional DTC and the proposed DTC based on combination of HCC and SVM are respectively shown in Figs. 6 and 7. For both techniques, the estimated stator flux magnitude is kept stable around 0.94 Wb with a little deviation obtained by the proposed DTC based on combination of HCC and SVM compared to the conventional DTC (Fig. 6a and Fig. 7a), it is clear that the motor speed is maintained close to its reference 2 880 rpm in steady state (Fig. 6b and Fig. 7b) and the estimated electromagnetic torque varies around 0.6 Nm for no-load case and 4 Nm for full load case with smaller oscillations in case of the proposed DTC based on combination of HCC and SVM compared to the conventional DTC case (Fig. 6c and Fig. 7c). It is also well observed that during load changes at time 0.6 s, both techniques ensure good dynamic control with sufficient time responses.

Figures 8 and 9 show the stator current of a-phase waveforms and their harmonic spectrum in rated state respectively for the conventional DTC and the proposed

DTC based on combination of HCC and SVM. It is clear that the proposed DTC ensures more quasi-sinusoidal waveforms compared to the conventional DTC (Fig. 8a and Fig. 8b) with a total harmonic distortion THD calculated up to the 50th order equal to 11.42 % for the conventional DTC (Fig. 9a) and 6.62 % for the proposed DTC (Fig. 9b).

Table 2

Parameters of the induction motor

Ratings	Y/Δ 380/220 V, 2.2 /3.8 A, 50 Hz, 1kW, cosφ=0.83,
Stator resistance R_s (Ω)	5.65
Rotor resistance R_r (Ω)	4.32
Mutual inductance L_m (mH)	725
Stator inductance L_s (mH)	737
Stator leakage inductance L_{ls}	12
Rotor inductance L_r (mH)	737
Inertia J (kg.m²)	0.0027
Friction coefficient f	0.00258

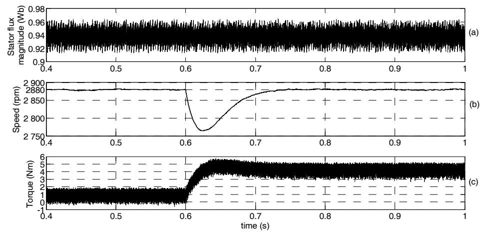

Fig. 6 – Simulation results during a load impact for the conventional DTC: a) estimated stator flux magnitude; b) motor speed and c) estimated electromagnetic torque.

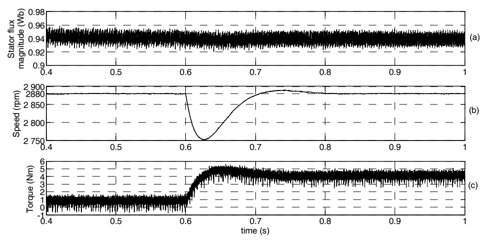

Fig. 7 – Simulation results during a load impact for the proposed DTC based on combination of HCC and SVM: a) estimated stator flux magnitude;b) motor speed and c) estimated electromagnetic torque.

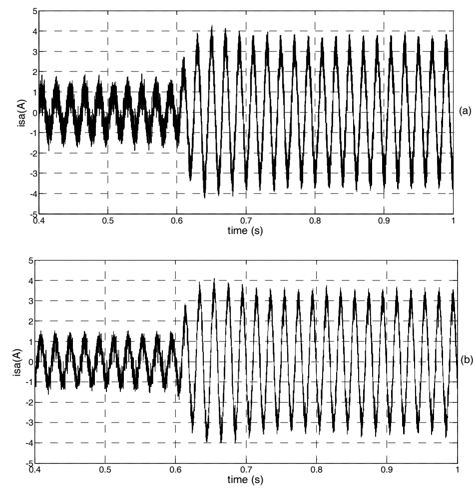

Fig. 8 – Stator current waveform: a) Conventional DTC and b) proposed DTC based on combination of HCC and SVM.

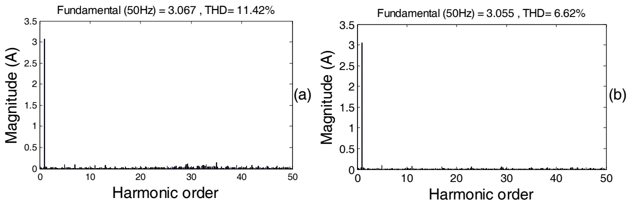

Fig. 9 – Harmonic spectrum of a-phase stator current: a) Conventional DTC and b) proposed DTC based on combination of HCC and SVM.

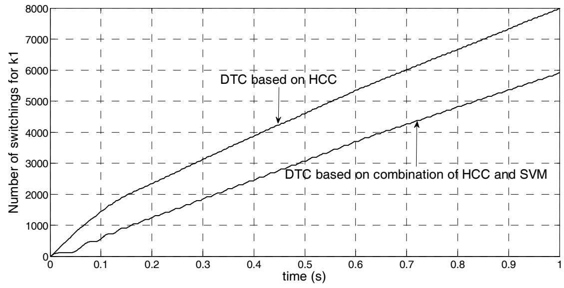

Fig. 10 – Number of switchings for K_1.

Figure 10 shows the number of switchings calculated on the interval [0 1 s] for the switch K_1 in the case of DTC based on HCC and DTC based on combination of HCC and SVM. The number of switchings in the proposed DTC based on combination of HCC and SVM is significantly reduced (about 26 %) compared to the DTC based on HCC with the same hysteresis band.

6. EXPERIMENTAL SYSTEM AND RESULTS

An experimental prototype has been developed in laboratory to examine the operating characteristic of the proposed DTC based on combination of HCC and SVM for induction motor. A three phase insulated gate bipolar transistor (IGBT) based inverter (SEMIKRON) is connected with a supply dc bus voltage generated by three-phase diode-bridge rectifier through three-phase ac supply. To ensure the insulation and the dead-time of control signals an integrated card is used. Two Hall-effect current sensors and one voltage sensor are employed to detect the stator currents and the dc bus voltage of inverter respectively and a speed sensor is used to detect the motor speed. The control program is written in MATLAB/Simulink real time interface with sampling frequency of 20 kHz and is implemented in real-time with dSPACE (RTI1104) digital signal processor installed in a PC Pentium. Several tests, in real-time implementation, were conducted to confirm the obtained simulation results. For these experimental tests, the same control data are used than in digital simulation tests.

Firstly, in order to better appreciate the static performance in rated state of the proposed DTC based on combination of HCC and SVM compared to the conventional DTC, the motor drive operates in steady state at rated speed 2 880 rpm with full load. The inverter is connected with a supply dc bus voltage of 630 V. During the application of these techniques, a power and quality analyzer instrument is used to obtain and examine the stator currents waveforms quality. These experimental electrical quantities allow to fairly compare the two techniques in steady state. Indeed, Figs. 11 and 12 show the stator current waveforms and the harmonic analysis of a-phase stator current for the conventional DTC and the proposed DTC respectively. It is clear that nearly sinusoidal stator current waveforms are achieved for the proposed DTC compared to the conventional DTC. It can be seen that the proposed DTC improves noticeably the quality of stator currents; this improvement is also explained by the reduction of THD (16.9 % for the conventional DTC and 7.3 % for the proposed DTC).

Secondly, since the very important features of the proposed DTC in comparison with conventional DTC are performance in steady state, in order to better appreciate this importance, different experimental waveforms are obtained in steady state with full load at low speed regions. Figure13 shows the stator current waveforms for the conventional DTC and the proposed DTC for 200 rpm. These waveforms are obtained by digital oscilloscope. Compared to the conventional DTC, it is well observed that the proposed DTC ensures a good quality of stator current waveform even at low speed regions. This offers a minimum torque ripple.

Finally, four experimental tests are proposed to examine the performance of the proposed DTC in transient of the speed reversal operation with full load in low speed regions: +500 rpm to – 500 rpm (Fig. 14a), from –500 rpm to +500 rpm (Fig. 14b), from +200 rpm to –200 rpm (Fig. 14c) and from 200 rpm to +200 rpm (Fig. 14d), these tests show clearly the better performance offered by the developed DTC based on combination of HCC and SVM technique compared to the conventional DTC technique in transient state conditions and in low speed regions operation. The proposed DTC ensures a good regulation of the motor speed in steady state and the stator flux magnitude is maintained close to its reference value 0.94 Wb with good stability. The estimated electromagnetic torque ripple level is drastically reduced. For both techniques, the time responses in transient of the speed reversal operation is sufficient.

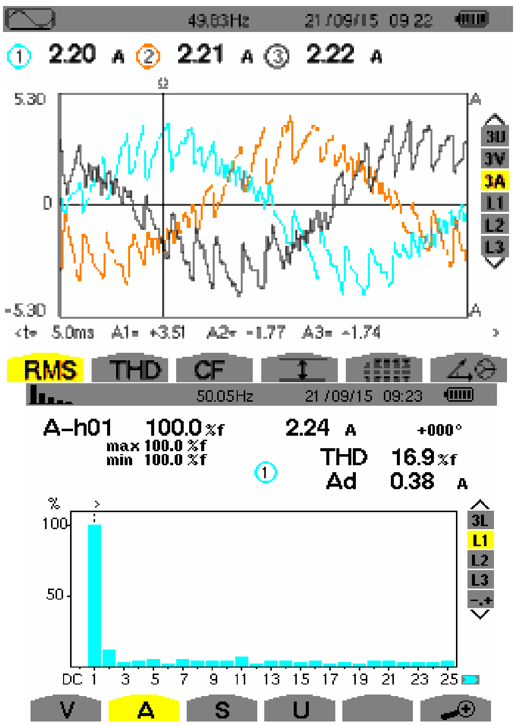

Fig.11 – Stator current waveforms and harmonic analysis of a-phase current stator for the conventional DTC.

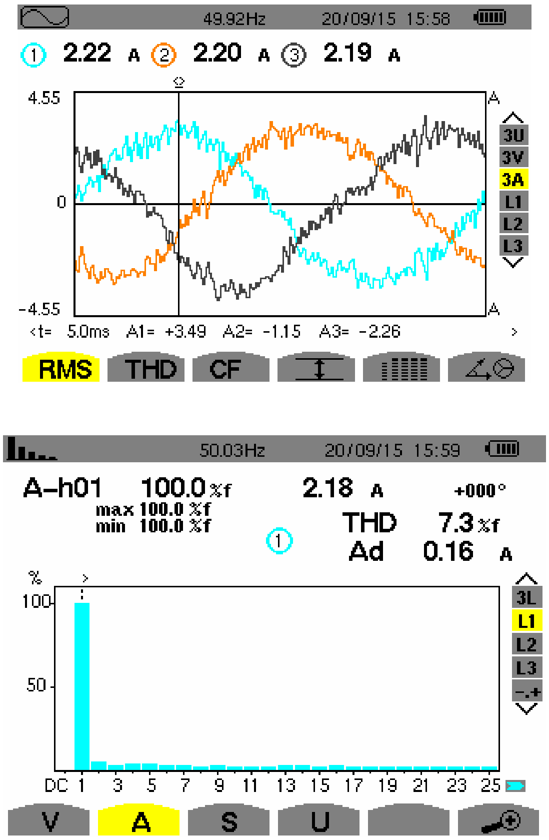

Fig. 12 – Stator current waveforms and harmonic analysis of a-phase current stator for the proposed DTC based on combination of HCC and SVM.

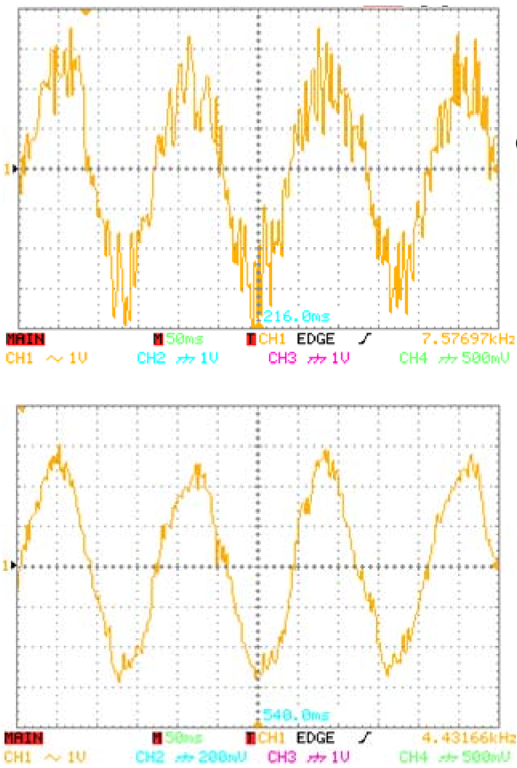

(a)

(b)

Fig. 13 – Stator current waveform for 200 rpm [1 A/div]: a) conventional DTC and b) proposed DTC based on combination of HCC and SVM.

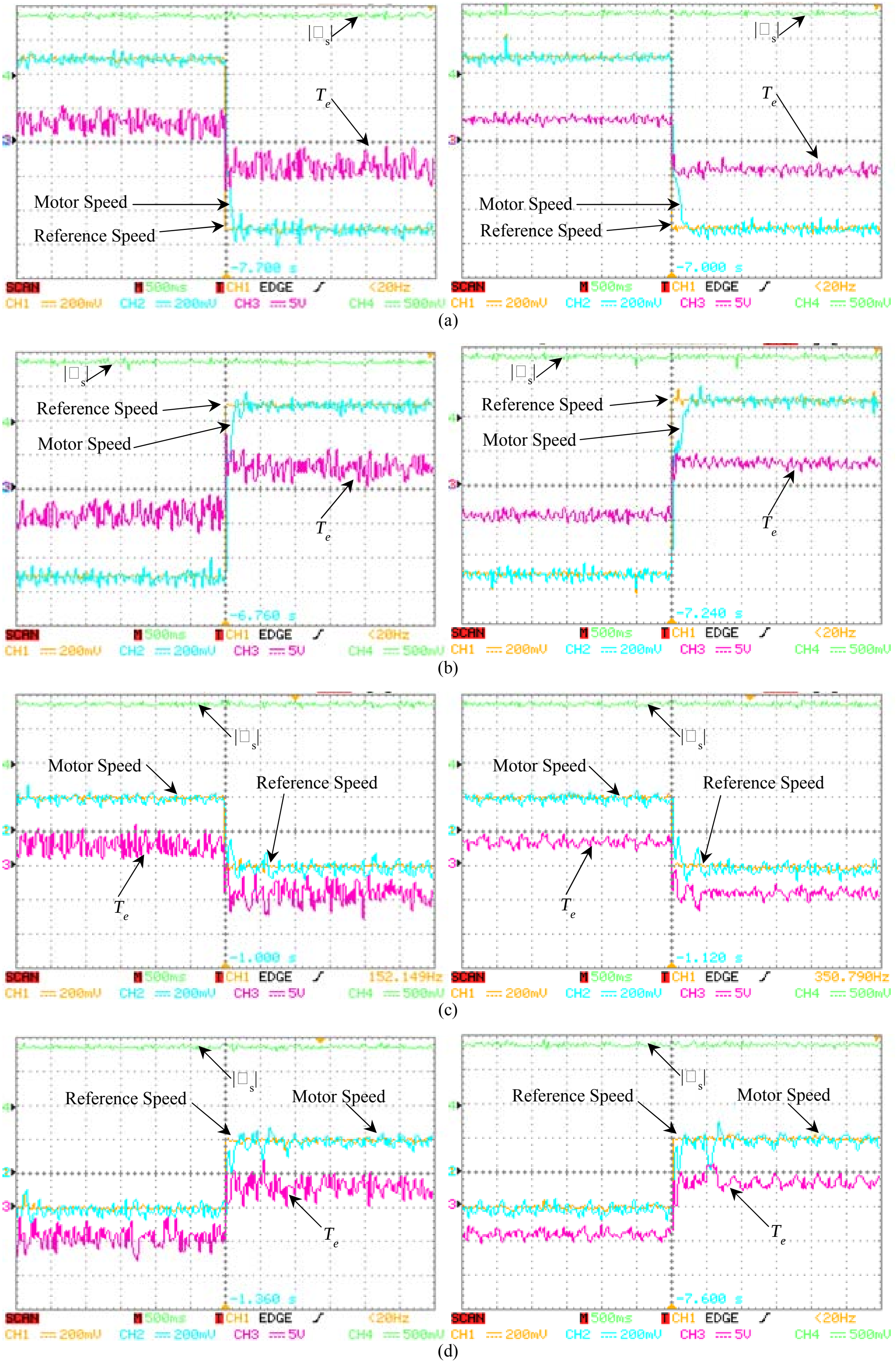

Fig. 14 – Experimental results during speed reversal operation: (left) conventional DTC and (right) proposed DTC based on combination of HCC and SVM, **(CHANNEL 1)** reference speed [200 rpm/div], **(CHANNEL 2)** motor speed [200 rpm/div], **(CHANNEL 3)** estimated electromagnetic torque [5 Nm/div], **(CHANNEL 4)** estimated stator flux magnitude [0.5 Wb/div]: a) from +500 rpm to –500 rpm; b) from –500 rpm to +500 rpm; c) from +200 rpm to –200 rpm; d) from –200 rpm to +200 rpm.

7. CONCLUSIONS

This paper has described a modified DTC based on combination of HCC and SVM technique for induction motor. The advantage of this modified DTC compared to the conventional DTC based on switching look-up table is to control not only the torque and the magnitude of flux but also the stator currents. This technique is characterized by simplicity and high robustness; it utilizes the advantages of the HCC and SVM techniques and leads to a significant reduction in the number of switchings compared to the DTC based on HCC.

The conventional DTC and the proposed DTC based on combination of HCC and SVM technique were simulated under Matlab/Simulink and implemented in real-time using dSPACE 1104 system card. It has been shown via simulation and experimental results that the proposed technique ensures a control of electromagnetic torque and stator flux with minimum ripple level and stator currents with high quality. The presented results indicate also that the combination of HCC and SVM in DTC can reduce the switching losses and the proposed DTC can improve ac drive performance noticeably particularly in steady state conditions.

Received on January 28, 2017

REFERENCES

1. Marcin Żelechowski, M. Sc, *Space vector modulated–Direct torque controlled (DTC– SVM) Inverter–fed induction motor drive*, Ph.D. Thesis, Warsaw University of Technology, 2005.
2. Giuseppe S. Buja, Marian P. Kazmierkowski, *Direct torque control of PWM inverter-fed AC motors–a survey*, IEEE Trans Ind Electron, **51**, *4*, pp. 744–757 (2004).
3. D. Casadei, G. Serra, A.Tani, *Implementation of a direct torque control algorithm for induction motors based on discrete space vector modulation*, IEEE Trans Power Electron, **15**, *4*, pp. 769–777 (2000).
4. N.R.N. Idris, A.H.M. Yatim, N.D. Muhamad, T.C. Ling, *Constant frequency torque and flux controllers for direct torque control of induction machines*, IEEE 34th Annual PESC'2003, Acapulco, Mexico, 19 June 2003, pp. 1095–1100.
5 M. Vasudevan, R. Arumugam, S. Paramasivam, *Real time implementation of viable torque and flux controllers and torque ripple minimization algorithm for induction motor drive*, ELSEVIER, Energy Conversion and Management, **47**, pp. 1359–1371 (2006).
6. Yuttana Kumsuwan, Suttichai Premrudeepreechacharn, Hamid A. Toliyat, *Modified direct torque control method for induction motor drives based on amplitude and angle control of stator flux*, ELSEVIER, Electric Power Systems Research, **78**, pp. 1712–1718 (2008).
7. Kuo-Kai Shyu, Juu-Kuh Lin, Van-Truong Pham, Ming-Ji Yang, and Te-Wei Wang, *Global minimum torque ripple design for direct torque control of induction motor drives*, IEEE Trans Ind Electron, **57**, *9*, pp. 3148–3156 (2010).
8. Auzani Jidin, Nik Rumzi Nik Idris, Abdul Halim Mohamed Yatim, Tole Sutikno, Malik E. Elbuluk, *An optimized switching strategy for quick dynamic torque control in DTC–Hysteresis–based induction machines*, IEEE Trans Ind Electron, **58**, *8*, pp. 3391–3400 (2011).
9. R. Abdelli, D. Rekioua, T. Rekioua, A.Tounzi, *Improved direct torque control of an induction generator used in a wind conversion system connected to the grid*, ISA Transactions(Elsevier), **52**, pp. 525–538 (2013).
10. Bhoopendra Singh, Shailendra Jain, Sanjeet Dwivedi, *Torque ripple reduction technique with improved flux response for a direct torque control induction motor drive*, IET Power Electron, **6**, *2*, pp. 326–342 (2013).
11. Tole Sutikno, Nik Rumzi Nik Idris, Auzani Jidin, Marcian N. Cirstea, *An improved FPGA implementation of direct torque control for induction machines*, IEEE Trans. Ind. Info., **9**, *3*, pp. 1280–1290 (2013).
12. Uday Kumar, V. Patil, Hiralal Murlidhar Suryawanshi, Mohan M. Renge, *Closed-loop hybrid direct torque control for medium voltage induction motor drive for performance improvement,* IET Power Electron, **7**, *1*, pp. 31–40 (2014).
13. Yongchang Zhang, Haitao Yang, *Model predictive torque control of induction motor drives with optimal duty cycle control*, IEEE Trans Power Electron, **29**, *12*, pp. 6593–6603 (2014).
14. J.A.T. Altuna, R.V. Jacomini, J.L.A. Puma, C.E. Capovilla, A.J. Sguarezi Filho, *Deadbeat controller applied to induction motor direct torque control with low-speed operation* (Springer), Electr. Eng., DOI 10.1007/s00202-016-0494-y (2016).
15. Q. Yao, D.G. Holmes, *A simple, novel method for variable–hysteresis–band current control of a three-phase inverter with constant switching frequency*, Proc. IEEE (IAS93) Ann. Meet. Conf. Rec., Toronto, 2–8 October 1993, pp. 1122–1129.
16. L. Sonaglioni, *Predictive digital hysteresis current control*, in Proc. IEEE (IAC), Orlando, FLUSA, 8–12 October 1995, pp. 1879–1886.
17. L. Malesani, P. Mattavelli, P. Tomasin, *Improved constant frequency hysteresis current control of VSI inverters with simple feedforward band with prediction*, IEEE Trans. Ind. Appl., **33**, *5*, pp. 1194–1202 (1997).
18. J. Zeng, C. Yu, Q. Qi, Z. Yan, Y. Ni, BL. Zhang, *A novel hysteresis current control for active power filter with constant frequency*, Electric Power Systems Research, **68**, pp. 75–82 (2004).
19. Bong-Hwan Kwon, Tae-Woo Kim, Jang-Hyoun Youm, *Novel SVM–based hysteresis current controller*, IEEE Trans Power Electron, **13**, *2*, pp. 297–307 (1998).
20. B.D. Min, J.H. Youm, B.H. Kwon, *SVM–based hysteresis current controller for three-phase PWM rectifier*, IEE Proc. Elec. Power Appl., **146**, *2*, pp. 225–230 (1999).
21. Keliang Zhou, Danwei Wang, *Relationship between space-vector modulation and three-phase carrier–based PWM: A comprehensive analysis*, IEEE Trans. Ind. Electron., **49**, *1*, pp. 186–196 (2002).